Hindawi
Advances in Meteorology
Volume 2017, Article ID 9156737, 11 pages
https://doi.org/10.1155/2017/9156737

Research Article

Temporal and Spatial Evolution Features of Precipitable Water in China during a Recent 65-Year Period (1951–2015)

Hao Wang[1] and Jianxin He[2]

[1]*College of Meteorological Observation, Chengdu University of Information Technology, Chengdu 610225, China*
[2]*Key Laboratory of Atmospheric Sounding, China Meteorological Administration, Chengdu 610225, China*

Correspondence should be addressed to Hao Wang; wh@cuit.edu.cn

Received 16 November 2016; Revised 24 February 2017; Accepted 14 March 2017; Published 26 March 2017

Academic Editor: Anthony R. Lupo

Water vapor in the atmosphere is not only an important greenhouse gas, but also an important factor that significantly affects the variations of global climate and water circulation. This study utilized the National Centers for Environmental Prediction (NCEP) and Climate Prediction Center Merged Analysis of Precipitation (CMAP) reanalysis data to probe the temporal and spatial distribution features of atmospheric precipitable water (PW) in China during a recent 65-year period (1951–2015), and the relationship between PW and actual precipitation was also studied. The temporal and spatial distribution characteristics of PW in China presented an overall decreasing spatial trend from the southeast to northwest direction. The spatial distribution pattern of the first eigenvector demonstrated that the PW in China shows nationwide variation features with a varying amount of PW across different regions. The year 1967 was further identified as an important transition period for the temporal and spatial distribution characteristics of the PW. We also found that the PW had inherent variability of around 30 years. Regarding the relationship with precipitation, PW was most closely correlated with precipitation in the northeastern region and the upper northwestern region in China. Different regions displayed different efficiencies for converting PW to precipitation. The conclusions are useful for understanding the long-term water vapor evolution and its potential effects on precipitation in China.

1. Introduction

Although there is only a small amount of water vapor in the atmosphere, it is one of the most active and important components [1, 2]. Water vapor plays a decisive role in sensible heat and latent heat transportation, cloud formation, and the occurrence of precipitation. In addition, as a greenhouse gas, water vapor plays a very important role in global climate change [3]. The content of water vapor in the atmosphere is often referred to as precipitable water (PW), which is defined as the depth of water in a column of the atmosphere. Variation of such data is usually indicative of the balance of water vapor in a certain area, and PW analyses play an important predictive role in regional precipitation forecasts, weather events, water circulation evaluations, and global warming analyses [4].

With the invention of the radiosonde in the 1950s, several domestic and foreign researchers began their studies on PW. Xu [5] calculated the water vapor transportation and water balance in July and January for eastern China with radiosonde and anemometric data from 1956 and discussed the differences in the sources and methods of water vapor transportation under different conditions in detail; Reitan [6] conducted a statistical analysis on the variation of monthly averaged PW in the continental USA during 1946 to 1956 with data from 52 radiosonde stations; Bannon et al. [7] studied the distribution of PW and water vapor transportation flux during winter and summer over the Northern Hemisphere with radiosonde data; and Wu [8] and Zheng and Yang [9] conducted notable studies on the distribution of PW in China. However, studies during this period mostly focused on the distribution features of PW. Since that time, more and more studies have emerged on the correlation between PW and actual precipitation as well as the external factors affecting the variation of PW. Wu and Shen [10] analyzed the content and transportation of water vapor during spring in China and their relationship

with rainfall in northern China; Zhou and Liu [11] analyzed the distribution of the average water vapor content in China and its controlling factors, and they discussed the distribution features and seasonal changes in the patterns of water vapor content. Zhai and Eskridge [12] used radiosonde data collected in China from 1970 to 1990 to examine the trends and variability of atmospheric water vapor content; they found that PW closely correlates with surface temperatures and precipitation in China. Though radiosonde data can provide information on PW over long periods, the scattered distribution of radiosonde stations prohibits detailed and accurate analyses of the evolution features of water vapor over large areas. With the development of science and technology, Askne and Nordius [13] raised the possibility of exploring the atmosphere with ground-based global positioning system (GPS) data in the late 1980s. As ground-based GPS can acquire atmospheric water vapor in all weather conditions and near real-time with high precision and temporal-spatial resolution, it has become an effective means for studies of atmospheric water vapor inversions. From the inversion of PW in the entire atmosphere [14, 15] to current studies of three-dimensional (3D) tomographic inversions [16, 17], ground-based GPS has played an important role as an independent data source in short-term forecasts, data assimilation procedures, and mode corrections [18]. Liang et al. [19] discussed the validity of using the Global Navigation Satellite System (GNSS) network to retrieve the precipitable water vapor (PWV) in China. Wang et al. [20] and Peng et al. [21] discussed interpolation schemes that can be used when GPS data are missing, which opened up possibilities for applying the GPS PWV data to climatological studies. Meanwhile, the development of additional types of detection equipment has allowed for the application of even more methods for the acquisition of PW. For example, Raman laser radar [22], ground-based sun photometer, and multifilter rotating shadowband radiometer (MFRSR) [23] techniques, as well as ground-based microwave radiometer technology [24], can all provide the distribution of PW. The main limitations of these technologies are that they are affected by working hours and weather conditions in ways that can lower their operability and shorten data accumulation times. With the rapid development of satellite remote sensing technology in the 1990s, the inversion of water vapor can now be realized with various detectors capable of measuring the thermal radiation or brightness temperature received by satellites via different channels. In regard to the inversion of PW, satellites can cover a broad range of areas with high spatial resolution, which is extremely significant and valuable in areas lacking observational data [25, 26]. However, because of limitations associated with their observation mode, satellites are unable to observe certain massive areas over long and continuous periods and many products have short data accumulation times over particular areas.

The above analysis indicates that certain observational means or methods tend to limit studies on long time series and large-scale PW trends, and most of the current studies on the variation features of PW in China have focused only on a certain area or a short period. Thus, such studies are incapable of expressing the overall nationwide features of PW in China; besides, certain studies based on radiosonde data can hardly be used to analyze the correlation between PW and precipitation because of the limitations posed by the layout of radiosonde stations, for which correlations can only be performed at certain points. On the basis of current studies and select research data, as well as new data sources, this study conducted an intensive analysis on the long-term spatial and temporal distribution features of PW in China, and the relationship between actual precipitation and PW was evaluated. The data sources and methods used are presented in Section 2, and the results and discussion material are presented in Section 3. The conclusions are presented in Section 4.

2. Data and Methods

The National Centers for Environmental Prediction/National Center for Atmospheric Research (NCEP/NCAR) reanalysis project is based on worldwide observation data that was jointly initiated by NCEP and NCAR in 1991. The data used in this project cover long periods of time with high spatial resolution and data continuity; in particular, the final output of reanalysis data consists of comprehensive results from various observational datasets and operational methods. The data are highly reliable because of the strict quality control procedures applied during the production of the output. The NCEP/NCAR reanalysis data assimilate data from 1948 to the present with the static analysis and forecasting system [27]. The NCEP data on PW are level-B data in the dataset according to the order of reliability, which means that such data are mainly based on actual observational data; in contrast, level-C data including data related to precipitation represent modeled data such as model-derived outgoing longwave radiation (OLR) or precipitation rates. Level-C data are considered to be less reliable as they are from model results and do not include observational data. Datasets with uniform spatial distribution and long-term coverage were obtained by the NCEP for PW through radiosonde observational techniques and multiple satellite remote sensing technology. These data served as the basis for this study on the spatial distribution features of PW in China. However, it should be noted that certain errors may occur during the application of NCEP data to PW analyses in certain areas [28, 29]. Zhao et al. [30] analyzed the NCEP reanalysis data for 1979–2012 and found that the data were highly correlated with the actual observational data from the perspective of climatological statistics (average value and spatial distribution); although there were certain errors in its description of PW in some regions in China, the pattern correlation remained at 0.97. The primary purpose of this study was not to study the absolute accuracy of the dataset but the long-term climate variations and temporal and spatial structural features. Therefore, such errors had less of an impact on the final results of this study. In this study, the data selected were the monthly averaged PW over a recent 65-year period from 1951 to 2015 that were provided by NCEP/NCAR at a spatial resolution of $2.5^\circ \times 2.5^\circ$. Chen et al. [31] assessed the ZTD (zenith tropospheric delay, which has a close relationship with the PW) of China and found that when the spatial resolutions of

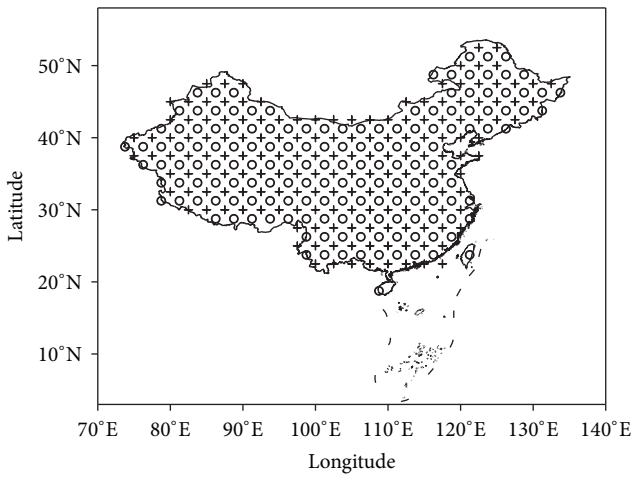

Figure 1: Distribution of grid-point locations for NCEP/NCAR PW (crosses) and CMAP precipitation (circles).

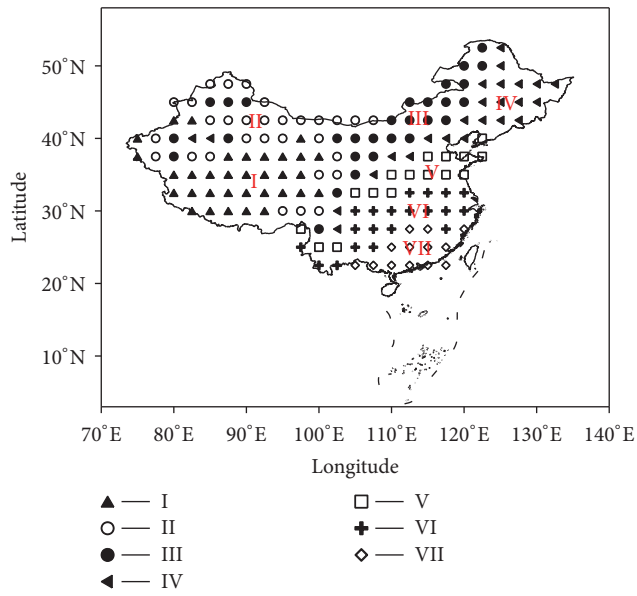

Figure 2: Grid-point classification results for PW.

the ECMWF (European Center for Medium-Range Weather Forecasts) meteorological data increase from 0.5° × 0.5° to 2.5° × 2.5°, the root-mean-square deviation (RMSD) for the ZTD only increases slightly. The results also show that the spatial scale of water vapor in China is slightly smaller than 2.5°. Thus, it is reasonable to analyze the PW database at a 2.5° × 2.5° spatial resolution. Liu et al. [32] successfully used PW from NCEP/NCAR with a 2.5° × 2.5° spatial resolution for studies in China; specifically, they validated the rationale of using data with this resolution for studying the spatial and temporal variations of PW by comparative analyses with radiosonde data. Together, these results demonstrate that the acquired data are applicable to analyzing the temporal and spatial variation of PW in China. The data on the monthly averaged precipitation for the comparative analysis came from the Climate Prediction Center Merged Analysis of Precipitation (CMAP) project [33, 34], and these data were available from January 1979 onward with the same spatial resolution of 2.5° × 2.5°. Specifically, such data were derived from the comprehensive results of four types of satellite products (GOES Precipitation Index (GPI), OLR Precipitation Index (OPI), Special Sensor Microwave/Imager (SSM/I) scattering data, SSM/I emission data, and microwave sounding unit (MSU) data). These data for precipitation are considered to be highly reliable, and, thus, they represent a highly effective means for conducting comparative analyses with other data [35]. The correlation study between the PW and precipitation was conducted with data collected during the same period. The distribution of grid-point locations for the selected PW and precipitation data in China is shown in Figure 1.

To further examine the variation of PW in each region with time, the PW in each region should be studied separately. While analyzing the PW in China, Zhai and Eskridge [12] also studied the zonal bands of PW across China. The regions were classified by their differences in geographical locations. However, such classifications may be subjective and can make the results unrepresentative for variations of PW, which do not have absolute geographical boundaries. Therefore, the dynamic clustering method based on the projection pursuit technique was adopted in this study for classifications according to the monthly variation features of PW in each grid-point [36]. The subjectivity caused by artificial classifications was thus avoided since the clustering results were completely data-driven. Such results can more reasonably reflect different variation features of PW. According to the dynamic clustering method, which requires the samples to have a maximum intraclass distance and minimum interclass distance, the optimal clustering results could be obtained when the clustering number was 7. Thus, all regions of China were divided into seven groups as shown in Figure 2; these groups included the Qinghai–Tibet Plateau region (region I), the northwestern region (region II), the northern region (region III), the northeastern region (region IV), the Yellow River basin region (region V), the Yangtze River basin region (region VI), and the South China region (region VII).

This study utilized a variety of analysis techniques. The temporal and spatial variation features of PW were first analyzed, followed by the time-space separation analyses conducted by a decomposition method that employed empirical orthogonal functions (EOFs) with the data for the monthly averaged PW over the 65-year period [37]; this method uses statistical analysis results to represent the variability distribution structure of PW in China to the utmost accuracy through the first few eigenvectors identified in significance tests. The Mann–Kendall test [38, 39] was employed to determine significant times of abrupt change in PW within the entire time series. External factors that may affect the variation of PW were eliminated based on time series decomposition [28] so that we could discern the inherent variation features of PW. Lastly, singular value decomposition (SVD) [40] was employed to study the relationship between precipitation and PW; this method diagonalizes the cross-covariance matrix

of the PW field and actual precipitation field to explain the variance of data fields with a few eigenvectors, which allows for the efficient study of the correlation between PW and precipitation.

3. Results and Discussion

3.1. Spatial Distribution Features of PW. Figure 3(a) shows the distribution of the annual averaged PW in China from 1951 to 2015. In general, the values for PW were high in the southeastern coastal areas and low in the northwestern inland areas, and the values progressively decreased in the southeast to northwest direction. Zheng and Yang [9] believe that this is mainly an outcome of the general temperature distribution and distance from water vapor sources. Figure 3(a) clearly indicates that a southwest–northeast moist tongue in South China is transported through the South China Sea to the mainland. The maximum values of PW were located in the southern regions of South China, and the annual averaged PW in this region exceeded 480 mm. Zveryaev and Chu [35] discovered through their work that the reason PW in this area stays high is because of the formation and development of strong convective clouds in the intertropical convergence zone that covers this area. Furthermore, this work has revealed that the isolines are densely distributed in southwestern China, especially in the Yunnan–Guizhou Plateau and the eastern portion of the Qinghai–Tibet Plateau, which suggests that a strong gradient of variation in PW exists here because the terrain has a significant influence on the distribution of PW. The Qinghai–Tibet Plateau had the lowest PW values in China, and the annual averaged PW in this region was about 20 mm. Therefore, both geographic latitude and altitude likely had a significant influence on the distribution of PW. The spatial distribution of PW in China shown in Figure 3 is largely consistent with that obtained by Zhai and Eskridge [12] and Xie et al. [41], whose work was based on radiosonde data, as well as that obtained by Wong et al. [42], whose work was based on GPS data.

The corresponding standard deviation (SD) of each grid-point (Figure 3(b)) was calculated based on the data for the monthly averaged PW to present the overall variation amplitude of PW in each region. It can be noticed from these results that the distribution features of the variability and the annual average distribution features of PW in China were basically consistent in the western region; that is, the regions with lower annual PW also had smaller variability. However, such a congruent relationship was not detected in the eastern region of the Chinese mainland, especially in the area east of South China, the Jianghuai basin (Yangtze River–Huaihe River basin), North China, and the northeastern region, which are all the regions with relatively high PW variation. The West Pacific subtropical high has a significant influence on the climate in China, and it is one of the most analyzed weather systems for weather forecasts in summer; the seasonal variation of its ridge corresponds to the seasonal displacement of the primary rain zone in the eastern region in China [43], which could explain some of the results obtained in this study. The north side of the subtropical high consists of mid-latitude westerlies and also a subtropical frontal zone. The southerly airflow in its western parts brings in abundant water vapor from the sea, where the water vapor is transported to the low levels of the frontal zone; these processes thus form a warm moisture conveyor in the western to northern boundary regions of the subtropical high that continuously transmits hot and humid airflow to the frontal zone on the north side of the subtropical high. Consequently, substantial accumulations of water vapor occur in this region. On average, the high ridge in May is located at around 15°N and the main rain band is located in South China. The ridge typically passes through 20°N in June, which is when the main rain band is located at the middle and lower reaches of the Yangtze River and Huaihe River basins. This induces a mold and rain period in the regions around the Yangtze River and Huaihe River basins. The ridge shifts to the north and passes through 25°N in the middle of July, with the main rain band moving to the Yellow River basin, thereby marking the beginning of the rainy season in North China. The area, intensity, northern and southern locations (northern boundary or ridge), and eastern and western advance and retreat of the West Pacific subtropical high all contribute to the determination of the course of the East Asian monsoon and associated mold-inducing rains; this is especially the case for the distribution of precipitation in the Yangtze River basin and the droughts and floods in North China and South China. Thus, the subtropical high has a significant influence on the distribution of water vapor in this region in summer, and changes in the system can lead to increases in the variability of PW, which is especially evident in the Jianghuai region.

The EOF decomposition analysis was conducted on the monthly averages to examine the interannual variability of PW in China. The results indicate that the variance contributions of the first and second vectors were 45.2% and 18.4%, respectively. According to Figure 4(a), the first vector was positive in most parts of China (except the Yunnan–Sichuan Plateau). Such a distribution pattern indicates that the PW in China has nationwide variation features, where the largest annual variability of PW is found in North China. The value is also generally characterized by a gradual increase across latitude, which indicates that the characteristics where the amount of PW in China deviates more from the mean value become more significant with the increase in latitude. In addition, the time coefficients that correspond to eigenvectors represent the temporal variation characteristics of the distribution patterns characterized by the eigenvectors in the region. As shown in Figure 5(a), the time coefficients were positive from 1951 to 1967 and were the largest in 1953. This indicates that most parts of China experienced a relatively high amount of PW during this time period, whereas the Yunnan–Sichuan Plateau experienced a distribution pattern with a relatively low amount of PW. In contrast, the time coefficients after 1967 were negative except for 1998 (Zhao et al. [44] found that the changes around 1997/1998 were associated with the strong El Niño at that time). From the time coefficients trend during 1951–2015, we found that this positive distribution pattern was more significant before 1967 (as reflected from a relatively larger absolute value for the time coefficient), whereas the opposite distribution pattern was observed afterward with less significant distribution

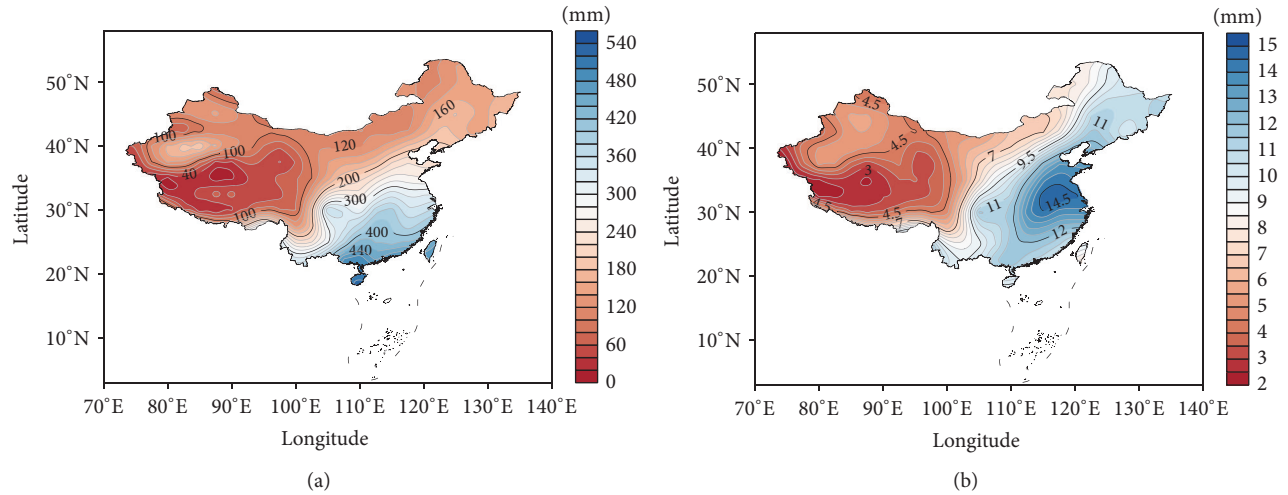

Figure 3: (a) Distribution of annual PW from 1951 to 2015 in China; (b) is similar to (a), but the data shown for the annual average PW are standard deviations.

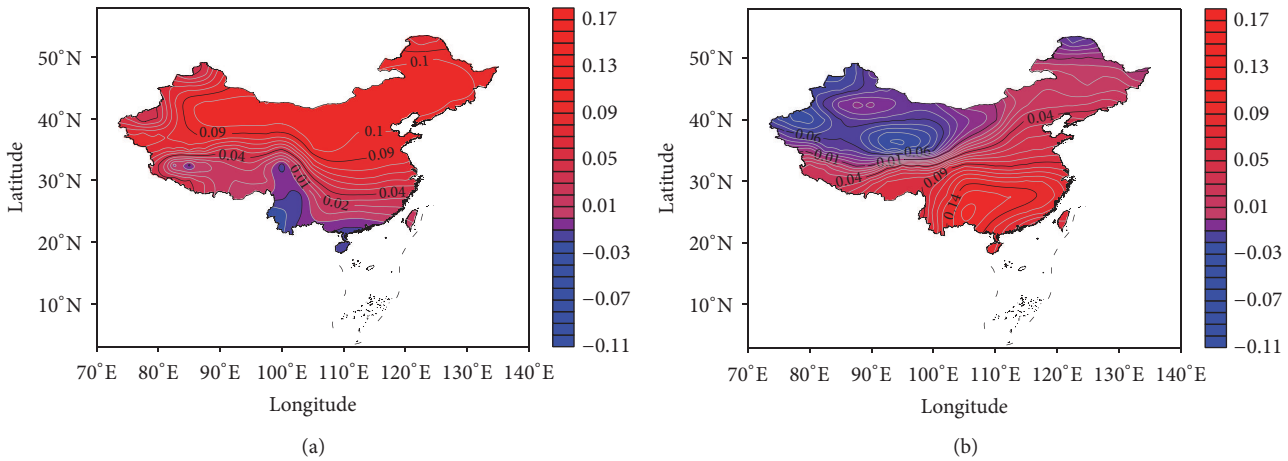

Figure 4: Distribution pattern of the (a) first and (b) second eigenvector of PW.

characteristics. Hence, 1967 is considered as an important transition period for the spatial distribution characteristics of the PW amount in China. The distribution pattern is similar to that in the study by Zhao et al. [30] who employed NCEP/NCAR reanalysis data from 1979 to 2012 to learn about the distribution patterns of PW in China, but the results are different in the region that contributed most to the variance. Such a difference might have been caused by the different time lengths of the selected data under study. As the annual amount of PW showed a gradual increase from north to south (apart from the Qinghai–Tibet Plateau region) and taking into account the distribution of the first eigenvector and first time coefficient, it can be interpreted that the difference in the PW amount between the north and south was larger before 1967 and smaller afterward, though an increasing trend for this difference was also observed after 2000. In contrast, the second eigenvector shows a dipole mode and displayed an opposite distribution pattern in Northwest China and other areas of China (Figure 4(b)), and this trend was more significant in the early 1960s (Figure 5(b)). From the change in the second time coefficient, there appears to be no significant trend in the difference between the PW amounts in Southeast and Northwest China, except in the early 1960s, when this difference was found to be more significant.

3.2. Temporal Variation Features of PW. The Mann–Kendall method [38, 39] was adopted for the further statistical analyses and tests of the variation trends for the time series of the annual average PW of China. This method is a nonparametric statistical test that is advantageous to use because it does not require the samples to exhibit a certain distribution; moreover, the results are not seriously affected by a small number of outliers. It is also more suitable for the ordinal variables. This method creates a rank statistic for a given sequence $x(t)$ $(t = 1, 2, \ldots, n)$ (where n is the number of samples, thus $n = 60$ in this paper), while the forward U-curve (UF) and backward U-curve (UB) are generated from the time series. When the absolute value of U is larger than 1.96, the sequence is said to have a nonrandom trend (0.05 significance level) [45, 46]. According to the curve

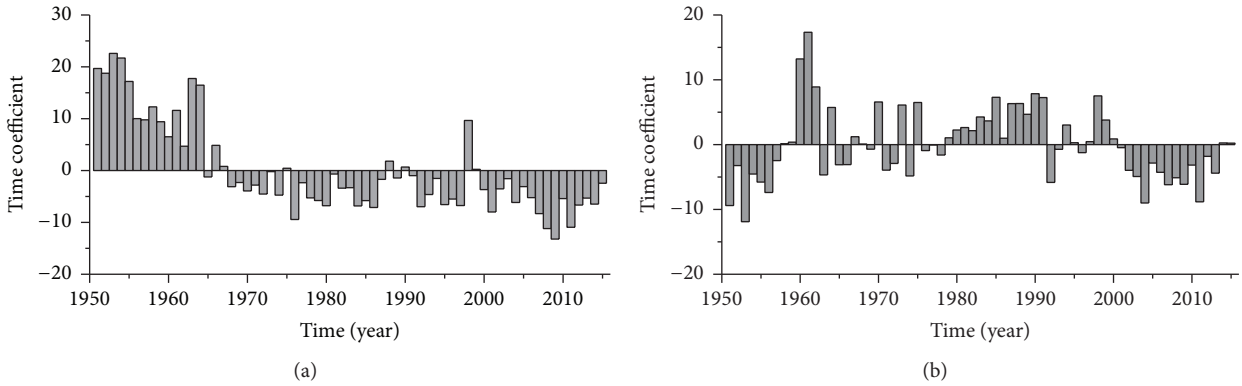

Figure 5: Time coefficients corresponding to the (a) first and (b) second eigenvector.

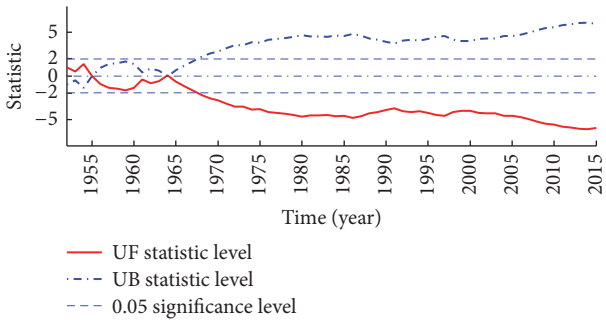

Figure 6: Mann–Kendall test results for the time series of annual average PW in China.

for the UF statistic shown in Figure 6, the PW in China displayed an overall decreasing trend starting in the middle to late 1950s, and such a trend was highly significant at the significance level of 0.05 from the 1960s to the middle 2010s. From these data, it can be concluded that an abrupt decrease of PW occurred in China in 1955, and the findings revealed the presence of a significant trend mutation with the year 1955 as the mutation point. It was also observed that the trend was not significant prior to 1967. The downtrend only became more evident after 1967 (exceeding the significant level of 0.05). Therefore, 1967 appears to represent a transition period when PW turned from a plentiful to scant resource. Considering the conclusion we obtained in Section 3.1, where the PW amounts in most parts of China after 1967 were found to be significantly less than normal, the year 1967 can be confirmed as an important transition period for the temporal distribution characteristics of PW in China.

On this basis, the variation trends of PW in the seven regions over the last 65 years were calculated (Table 1). Decreases were most evident in the northwestern, northern, and northeastern regions of China, and such a decrease was most pronounced in the northwestern region.

The synthetic analysis method was utilized to further study the monthly average variation of PW in each region [4]. This method involved adding up the annual monthly PW amounts from the different regions in the last 60 years and computing the average, which resulted in the monthly average values of the PW amount. According to the distribution features of the monthly averaged PW during the 65-year period (Figure 7), the Qinghai–Tibet Plateau region had the lowest amount of PW in China with an annual average of 3.91 mm, while South China had the highest amount, which was over 9 times that in the Qinghai–Tibet Plateau region. The PW in the seven regions basically increased from January to July in each year and then decreased from July to December; thus, the amount of PW was the highest in summer and the lowest in winter. The PW in the southern regions was much greater than that in the northern regions. Though different regions had different amounts of PW, the regions showed quite similar variation trends for the monthly averaged PW with each passing year, thus indicating that the variation of PW is controlled by the periodical variation of a larger system. Zheng and Yang [9], Zhai and Eskridge [12], and Zhao [47] all noted that the variation of PW is closely associated with the variation of temperature in China. Wang et al. [4] proposed that the significant seasonal differences in PW are mainly due to the different amounts of transported water vapor, which fluctuate in accordance with variations in the intensity of meridional and zonal winds. Since there are various factors affecting the variation of PW, it is difficult to identify the primary factor that determines its variation via limited data. Therefore, this issue still requires further exploration.

Since PW varies significantly with the seasons, the seasonal variation trend should be eliminated in order to further study the actual variation of PW. In this paper, the multiplicative model of time series analysis [28] was adopted to decompose the PW in each season in China to obtain the seasonally adjusted series, seasonally adjusted factors, and residual factors. The seasonally adjusted series were smoothed (the smoothening was achieved by calculating the moving average when all the points were within an equal span with each other and with an equal weighting) and the magnitude trend was detrended to obtain the PW internal variation tendency as shown in Figure 8. When the Fast Fourier Transform (FFT) was further applied to that particular time series [4], it was found that the most powerful cycle of the series was 30 years. Taking 30 years as the demarcation point, the series were divided into three cycles,

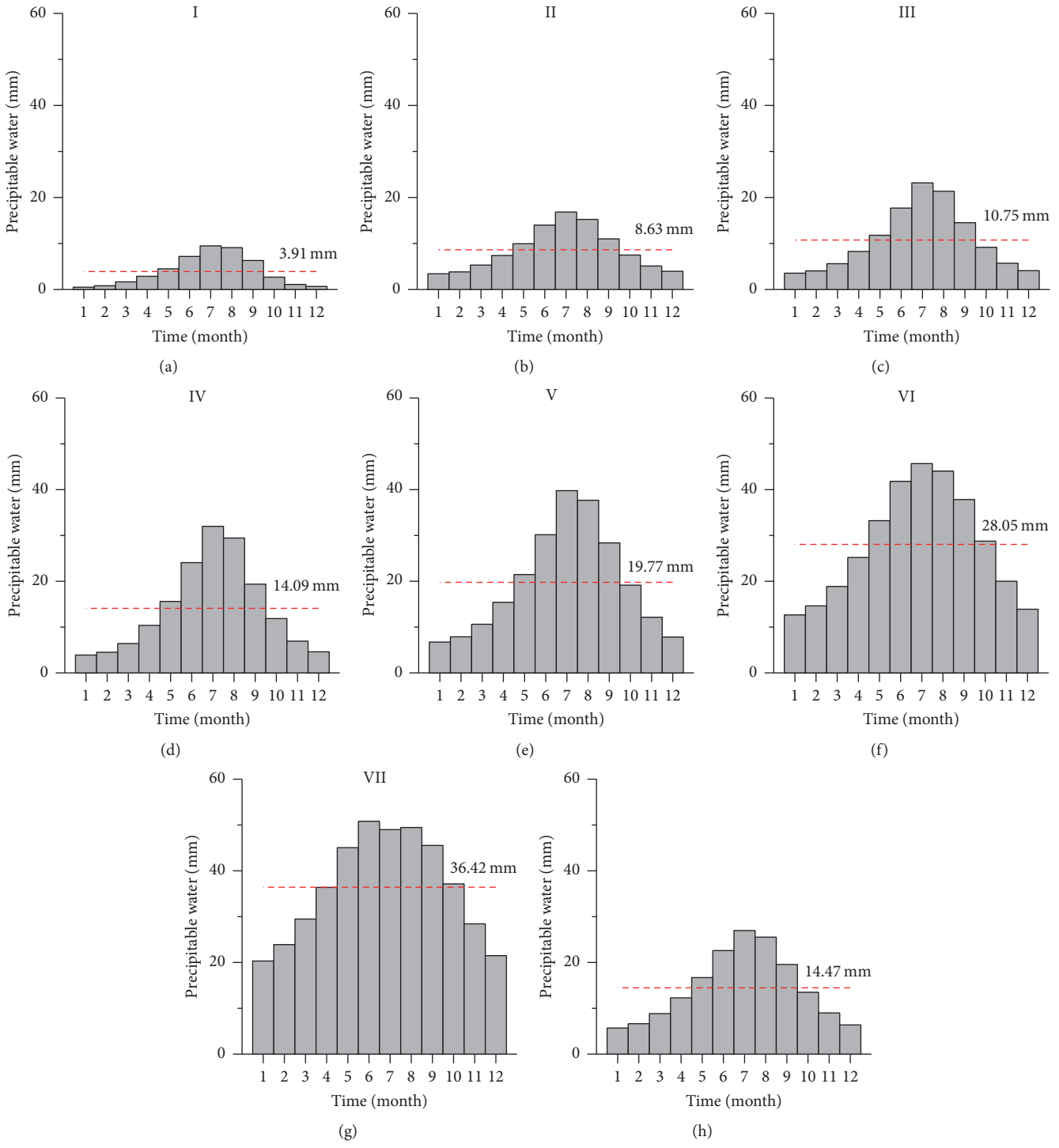

Figure 7: Monthly average PW from January to December during 1951 to 2015. (a)–(f) denote monthly average PW from region I to region VII and (h) represents the monthly average PW in China. The red dashed line in (a)–(h) depicts the average annual precipitation atmospheric precipitable amount in each region.

Table 1: Statistics for the variation trends of PW in different regions.

District	I	II	III	IV	V	VI	VII
Rate of change (mm/decade)	−0.3447	−0.6319	−0.4859	−0.4746	0.01	−0.3259	−0.1772

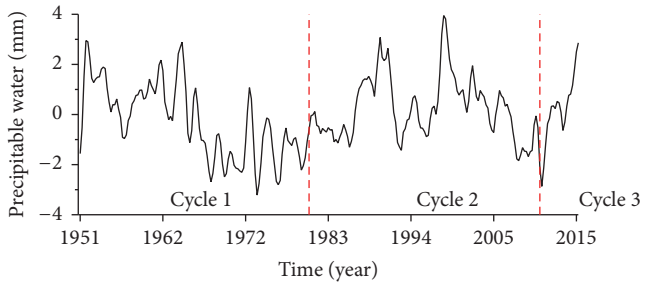

Figure 8: Time series of PW excluding the trend features after seasonal adjustments and smoothness procedures were applied (calculated with season as the basic unit).

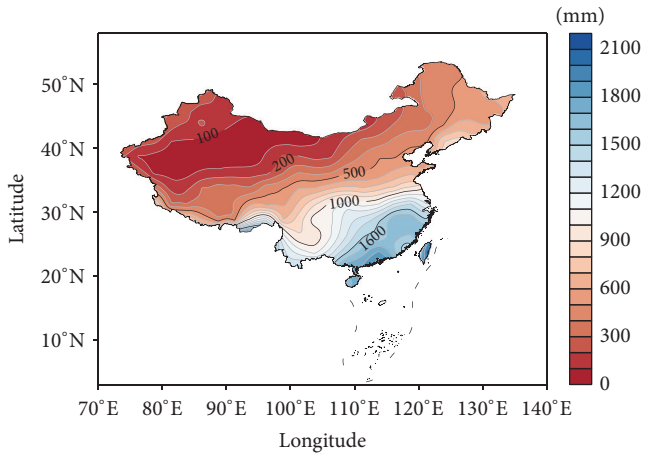

Figure 9: Distribution of annual average precipitation in China from 1979 to 2015.

namely, Cycle 1, Cycle 2, and the incomplete Cycle 3. For each cycle, the first half of it (around 15 years) basically presented an obvious upward trend while the second half presented a downward trend, whose start times coincided with the times of overall significant decreases of PW in China; given the variations of both the external trend of PW and its own trend, these points in time represent a significant turning point. If the analysis is conducted according to this cycle, the PW in China in the next decade is going to have an overall upward trend excluding the influence caused by external factors (e.g., seasonal variation factors and trend factors).

3.3. Correlation Features of PW and Actual Precipitation. The influential effect of PW on actual precipitation is the focus of the following research. The CMAP data on the monthly averaged precipitation were adopted to calculate the distribution of annual averaged precipitation in China. Figure 9 shows the distribution of annual averaged precipitation in China from 1979 to 2015.

According to Figure 9, the precipitation in mainland China progressively decreases in the southeast to northwest direction. The maximum precipitation amounts were located in South China where the annual average precipitation was over 1,600 mm; the minimum precipitation amounts were located around Northwest China where the annual average precipitation was less than 100 mm. Such distribution features are largely consistent with those for the annual averaged PW in China, albeit some key differences do exist in certain areas; for example, the minimum value for PW was located in the Qinghai–Tibet Plateau, while the minimum value for actual precipitation was located in Northwest China.

Zhai and Eskridge [12] found that the PW in China is closely correlated with actual precipitation (the correlation coefficient was 0.64), but the timescale of their statistical analysis was relatively short (the data coverage was from 1970 to 1990). Zhao et al. [1] also found that these variables are closely correlated, but their variations were inconsistent to a great extent because of regional climate variations. Therefore, to obtain the correlation between PW and actual precipitation in different regions over a longer period of time and to investigate the influencing mechanism, this study adopted the SVD [48] method. As this method can maximize the separation between the highly correlated areas of two variable fields, which can be interpreted as the contributions to the spatial structures of the correlation coefficient fields between the variable fields and the contributions to the corresponding correlation coefficients, the SVD method can be used as a diagnostic tool for studying the interrelationships between two meteorological variable fields [49]. By extracting the relevant patterns with the SVD method, this study performed SVD separation on the PW amounts and the precipitation data of China to obtain the typical spatial distribution pattern resulting from the interaction between the PW amount and the actual precipitation. In this study, we selected the average monthly precipitation data in China obtained during 1979–2007 and with a spatial resolution of 2.5° × 2.5° as one of the variable fields, which is referred to as the left field in this paper; it has a total of 158 grid-points. The average monthly PW data of the same period and with a spatial resolution of 2.5° × 2.5° were selected as the other variable field, which is referred to as the right field in this paper; it has a total of 166 grid-points. The SVD calculations were performed after standardizing the two variable fields. Figure 10 shows the spatial distribution patterns of the left and right anisotropic correlation coefficient field of the first model, for which the variance contribution was 99.78%, a far greater value than that of the other models. The correlation coefficient between the two fields was determined to be 0.97, which is also the correlation coefficient of the time coefficients of the spatial distribution pattern of the pair. This indicates that the spatial distribution patterns of the pair were closely related to each other, which further indicates that the change in PW amount was closely related to the actual precipitation amount. Furthermore, the variance contribution of the left field was 58%, while that of the right field reached 93%, which indicates that the change in PW amount had a dominating effect on the interaction between the two. The SVD spatial distribution pattern of the anisotropic correlation coefficient field of the first model's right field also indicated that the PW amount and the precipitation amount were positively correlated with each other. This was especially the case in the northeast region and the northern part of the northwest region of China, where the anisotropic correlation coefficient of the right field was over 0.96 and reached a 0.001 significance

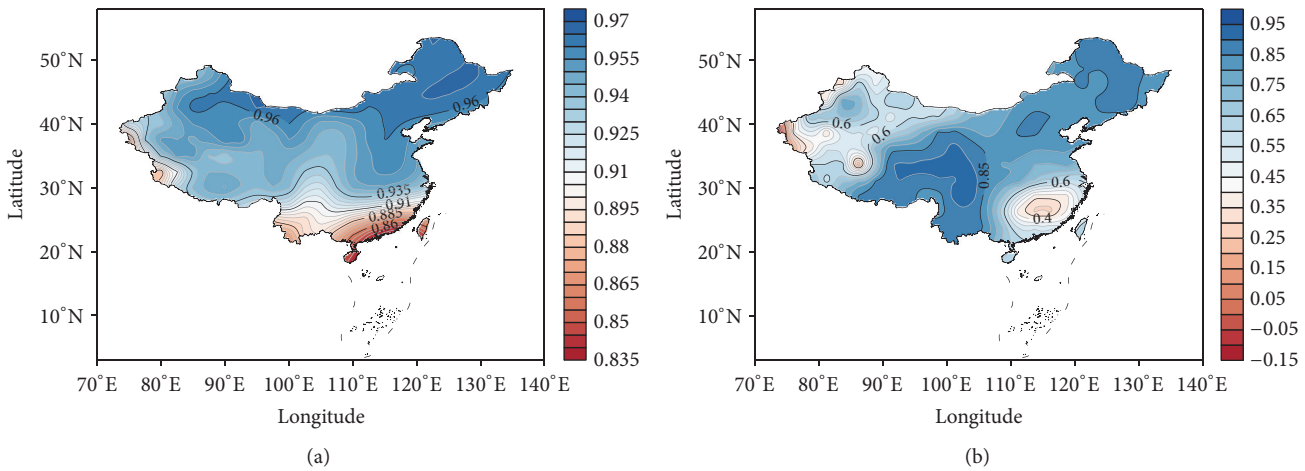

Figure 10: The SVD distributions of PW and precipitation in China: (a) distribution of anisotropic correlation coefficients for the right field of the first model and (b) distribution of anisotropic correlation coefficients for the left field of the first model.

level. Such a finding indicates that PW was closely related to precipitation in areas with high isolines, and as this high correlation was represented by static absolute values and dynamic features of variation with time; it also indicates that PW can be transformed into precipitation more efficiently. In contrast, PW was less closely related to actual precipitation in South China where high PW was present, which was possibly because of the strong convective activities that are common in the coastal area and the abundant water vapor that varies greatly in the atmosphere [18]. Harrison [50] found in his study on the relationship between PW and actual precipitation in the inland region of central South Africa that PW decreases the efficiency of precipitation after exceeding a certain threshold; thus, regions with higher PW may not have the highest precipitation rate. Consequently, PW is likely not a good indicator of actual precipitation under such conditions. The distribution features of the anisotropic correlation coefficients of the left field can also reflect the feedback effect of precipitation on PW, and such feedback was even more significant in the northeastern and southwestern areas of China. Besides, evaporation from the ground can have a positive effect on the accumulation of PW. The findings also suggest that areas with high and low precipitation can have an insignificant feedback effect on the occurrence of PW. Zhai and Eskridge [12] also studied the interaction effect between PW and actual precipitation obtained by radiosonde data and proposed that such an effect is possibly due to the fact that both PW and actual precipitation are under the control of the same atmospheric dynamic conditions.

4. Summary

This study conducted an intensive analysis on the spatial and temporal distribution features of PW in China during a recent 65-year period (1951–2015) based on NCEP reanalysis data, and, furthermore, the correlation between the PW data and precipitation data provided by CMAP was investigated. As a result of this research, the following conclusions were reached:

(1) Spatial Distribution Features of PW. High values of PW were common in the southeastern coastal area of China, while low values were common in the northwestern inland area. There was a general and progressive decrease in PW in the southeast to northwest direction. The spatial distribution pattern of the first eigenvector demonstrated that the PW in China had nationwide variation features. By considering the time coefficient corresponding to the first eigenvector, it was found that the year 1967 was an important transition period for the spatial distribution characteristics of the PW amount in China.

(2) Temporal Variation Features of PW. Through the Mann–Kendall mutation test, it was found that most parts of China exhibited a significant low in the PW amount after 1967, which indicates that the year 1967 was an important transition period for the temporal distribution characteristics of PW in China. It was also found that during the 65-year analysis period the decreases in PW were most evident in the northwestern, northern, and northeastern regions of China. In general, the PW increased gradually from January to July in each year and decreased gradually from July to December, and, thus, the highest amounts were observed in summer and the lowest amounts were observed in winter. Time series analysis was adopted in this paper and we found that during these 65 years the PW in China had a cycle of around 30 years (the influence of external factors was excluded in this particular analysis to reveal the inherent variations).

(3) Correlation Features of PW and Actual Precipitation. The PW had a decisive influence on the quantity and evolution of precipitation. The data showed that PW was closely related to precipitation in northeastern China and portions of northwestern China, and consequently, high correlations were detected between the static absolute values and also the dynamic features of variation with time; in these areas, PW was transformed into precipitation efficiently. In contrast, PW was less closely related to actual precipitation in South China where there was high PW. Hence, PW was not

transformed into precipitation efficiently in this region. On the other hand, precipitation did have a certain feedback effect on PW, and such an effect was most pronounced in the northeastern and southwestern parts of China.

As water vapor plays an important role in weather related processes and climate change, it is of great theoretical and practical significance to study its temporal and spatial evolution features. Studies have shown that knowledge of water vapor variation features can have a positive influence on forecasts of regional precipitation, early warnings of flood disasters, weather modification predictions, and assessments of regional water resources, particularly in areas with many flood related disasters. Though certain important conclusions have been drawn in this study, the evolution of PW in the future may not necessarily vary in accordance with the current development trends, and, thus, the focus of future studies should be on how to find the internal variation mechanism of PW and the key external factors that affect its variation. Besides, with further improvements in the temporal and spatial resolution of observational data and the availability of more and more observation means, studies on PW are expected to produce more elaborate results whereby judgments regarding the evolution of water vapor in three-dimensional space and its relation to actual precipitation will also be more accurate.

Conflicts of Interest

The authors declare that there are no conflicts of interest regarding the publication of this paper.

Acknowledgments

This work was supported by the National Natural Science Foundation of China (no. 41405036, no. 41471305), the 2015 Middle-Aged Academic Leaders Research Fund of Chengdu University of Information Technology (CUIT) (J201502), a Project of the Sichuan Education Office (15ZB0181), and the Scientific Research Foundation of CUIT (KYTZ201413). The authors would like to express their sincere thanks to the NCEP/NCAR and CMAP for supplying the relevant data.

References

[1] T. Zhao, K. Tu, Z. Yan et al., "Advances of atmospheric water vapor change and its feedback effect," *Advances in Climate Change Research*, vol. 9, no. 2, pp. 79–88, 2013 (Chinese).

[2] H. Wang, G. Chen, H. Lei, Y. Wang, and S. Tang, "Improving the predictability of severe convective weather processes by using wind vectors and potential temperature changes: a case study of a severe thunderstorm," *Advances in Meteorology*, vol. 2016, Article ID 8320189, 2016.

[3] B. Fontaine, P. Roucou, and S. Trzaska, "Atmospheric water cycle and moisture fluxes in the West African monsoon: mean annual cycles and relationship using NCEP/NCAR reanalysis," *Geophysical Research Letters*, vol. 30, no. 3, pp. 101029–101032, 2003.

[4] H. Wang, M. Wei, G. Li, S. Zhou, and Q. Zeng, "Analysis of precipitable water vapor from GPS measurements in Chengdu region: distribution and evolution characteristics in autumn," *Advances in Space Research*, vol. 52, no. 4, pp. 656–667, 2013.

[5] S. Xu, "Water vapor transfer and water balance over the eastern China," *Acta Meteor. Sinica*, vol. 29, no. 1, pp. 33–43, 1958 (Chinese).

[6] C. Reitan, "Distribution of PW vapor over the continental United States," *Bulletin of the American Meteorological Society*, vol. 41, no. 2, pp. 79–87, 1960.

[7] J. K. Bannon, A. G. Matthewman, and R. Murray, "The flux of water vapour due to the mean winds and the convergence of this flux over the Northern Hemisphere in January and July," *Quarterly Journal of the Royal Meteorological Society*, vol. 87, no. 374, pp. 502–512, 1961.

[8] B. Wu, "The average PW vapor over China," *Journal of Nanjing University (Natural Sciences)*, vol. 6, pp. 43–48, 1959 (Chinese).

[9] S. Zheng and D. Yang, "Distribution of precipitable water vapor over China," *Acta Geographica Sinica*, vol. 28, no. 2, pp. 124–136, 1962 (Chinese).

[10] Y. Wu and J. Shen, "The moisture content and it's transportation in spring over China and their correlation with the precipitation in north China," *Journal of Beijing Normal University*, vol. 3-4, pp. 123–129, 1980 (Chinese).

[11] J. Zhou and H. Liu, "The basic features of distribution of water vapor content and their controlling factors in China," *Acta Oceanologica Sinica*, vol. 36, no. 4, pp. 377–391, 1981 (Chinese).

[12] P. Zhai and R. E. Eskridge, "Atmospheric water vapor over China," *Journal of Climate*, vol. 10, no. 10, pp. 2643–2652, 1997.

[13] J. Askne and H. Nordius, "Estimation of tropospheric delay for microwaves from surface weather data," *Radio Science*, vol. 22, no. 3, pp. 379–386, 1987.

[14] M. Bevis, S. Businger, T. A. Herring, C. Rocken, R. A. Anthes, and R. H. Ware, "GPS meteorology: remote sensing of atmospheric water vapor using the global positioning system," *Journal of Geophysical Research*, vol. 97, no. 14, pp. 15–801, 1992.

[15] C. Rocken, R. Ware, T. Van Hove et al., "Sensing atmospheric water vapor with the global positioning system," *Geophysical Research Letters*, vol. 20, no. 23, pp. 2631–2634, 1993.

[16] J. Braun, C. Rocken, and R. Ware, "Validation of line-of-sight water vapor measurements with GPS," *Radio Science*, vol. 36, no. 3, pp. 459–472, 2001.

[17] L. P. Gradinarsky and P. Jarlemark, "Ground-based GPS tomography of water vapor: analysis of simulated and real data," *Journal of the Meteorological Society of Japan*, vol. 82, no. 1, pp. 551–560, 2004.

[18] H. Wang, J. He, M. Wei, and Z. Zhang, "Synthesis analysis of one severe convection precipitation event in jiangsu using ground-based GPS technology," *Atmosphere*, vol. 6, no. 7, pp. 908–927, 2015.

[19] H. Liang, Y. Cao, X. Wan, Z. Xu, H. Wang, and H. Hu, "Meteorological applications of precipitable water vapor measurements retrieved by the national GNSS network of China," *Geodesy and Geodynamics*, vol. 6, no. 2, pp. 135–142, 2015.

[20] H. Wang, D. Wang, and G. Li, "A method of inserting and mending for the GPS precipitable water vapor," in *Proceedings of the 2nd International Conference on Multimedia Technology (ICMT 11)*, pp. 3350–3353, July 2011.

[21] J. Peng, Y. Shirong, C. Dezhong et al., "Retrieving PW Vapor data using gps zenith delays and global reanalysis data in China," *Remote Sensing*, vol. 8, no. 389, pp. 1–21, 2016.

[22] D. N. Whiteman, S. H. Melfi, and R. A. Ferrare, "Raman lidar system for the measurement of water vapor and aerosols in the

earth's atmosphere," *Applied Optics*, vol. 31, no. 16, pp. 3068–3082, 1992.

[23] K. J. Thome, B. M. Herman, and J. A. Reagan, "Determination of precipitable water from solar transmission," *Journal of Applied Meteorology*, vol. 31, no. 2, pp. 157–165, 1992.

[24] F. Solheim, J. R. Godwin, E. R. Westwater et al., "Radiometric profiling of temperature, water vapor and cloud liquid water using various inversion methods," *Radio Science*, vol. 33, no. 2, pp. 393–404, 1998.

[25] P. Salio, M. P. Hobouchian, Y. García Skabar, and D. Vila, "Evaluation of high-resolution satellite precipitation estimates over southern South America using a dense rain gauge network," *Atmospheric Research*, vol. 163, pp. 146–161, 2015.

[26] S. Prakash, A. K. Mitra, D. S. Pai, and A. AghaKouchak, "From TRMM to GPM: how well can heavy rainfall be detected from space?" *Advances in Water Resources*, vol. 88, pp. 1–7, 2016.

[27] E. Kalnay, M. Kanamitsu, R. Kistler et al., "The NCEP/NCAR 40-year reanalysis project," *Bulletin of the American Meteorological Society*, vol. 77, no. 3, pp. 437–471, 1996.

[28] S. Vey, R. Dietrich, A. Rülke, M. Fritsche, P. Steigenberger, and M. Rothacher, "Validation of precipitable water vapor within the NCEP/DOE reanalysis using global GPS observations from one decade," *Journal of Climate*, vol. 23, no. 7, pp. 1675–1695, 2010.

[29] H. Wang, M. Wei, and S. H. Zhou, "A feasibility study for the construction of an atmospheric precipitable water vapor model based on the neural network technology," *Desalination and Water Treatment*, vol. 52, no. 37-39, pp. 7412–7421, 2014.

[30] T. Zhao, J. Wang, and A. Dai, "Evaluation of atmospheric precipitable water from reanalysis products using homogenized radiosonde observations over China," *Journal of Geophysical Research: Atmospheres*, vol. 120, no. 20, pp. 10703–10727, 2015.

[31] Q. Chen, S. Song, S. Heise, Y.-A. Liou, W. Zhu, and J. Zhao, "Assessment of ZTD derived from ECMWF/NCEP data with GPS ZTD over China," *GPS Solutions*, vol. 15, no. 4, pp. 415–425, 2011.

[32] D. Liu, X. Qiu, L. Shi et al., "Estimation of PW in China with NCEP data and its spatio-temporal distribution," *Journal of NUIST (Natural Science Edition)*, vol. 5, no. 2, pp. 113–119, 2013.

[33] P. Xie and P. A. Arkin, "Analyses of global monthly precipitation using gauge observations, satellite estimates, and numerical model predictions," *Journal of Climate*, vol. 9, no. 4, pp. 840–858, 1996.

[34] P. Xie and P. A. Arkin, "Global precipitation: a 17-year monthly analysis based on gauge observations, satellite estimates, and numerical model outputs," *Bulletin of the American Meteorological Society*, vol. 78, no. 11, pp. 2539–2558, 1997.

[35] I. I. Zveryaev and P.-S. Chu, "Recent climate changes in PW vapor in the global tropics as revealed in National Centers for Environmental Prediction/National Center for Atmospheric Research reanalysis," *Journal of Geophysical Research*, vol. 108, p. 4311, 2003.

[36] C.-J. Ni, S.-J. Wang, and P. Cui, "Projection pursuit dynamic cluster model and its application in groundwater classification," *Journal of Sichuan University (Engineering Science Edition)*, vol. 38, no. 6, pp. 29–33, 2006 (Chinese).

[37] K. Pearson, "On lines and planes of closest fit to systems of points in space," *Philosophical Magazine*, vol. 2, pp. 559–572, 1901.

[38] H. B. Mann, "Non-parametric tests against trend," *Econometrica*, vol. 13, no. 3, pp. 245–259, 1945.

[39] M. Kendall, *Rank Correlation Methods*, Charles Griffin, London, UK, 4th edition, 1975.

[40] C. Xingxin and C. Min, *Statistical Calculating Method*, Peking University Press, Beijing, China, 1989 (Chinese).

[41] B. Xie, Q. Zhang, and Y. Ying, "Trends in precipitable water and relative humidity in China: 1979–2005," *Journal of Applied Meteorology and Climatology*, vol. 50, no. 10, pp. 1985–1994, 2011.

[42] M. S. Wong, X. Jin, Z. Liu, J. Nichol, and P. W. Chan, "Multi-sensors study of precipitable water vapour over mainland China," *International Journal of Climatology*, vol. 35, no. 10, pp. 3146–3159, 2015.

[43] G. Wu, J. Chou, Y. Liu et al., "Review and prospect of the study on the subtropical anticyclone," *Journal of the Atmospheric Sciences*, vol. 27, no. 4, pp. 503–517, 2003.

[44] T. Zhao, A. Dai, and J. Wang, "Trends in tropospheric humidity from 1970 to 2008 over china from a homogenized radiosonde dataset," *Journal of Climate*, vol. 25, no. 13, pp. 4549–4567, 2012.

[45] D. Gellens, "Trend and correlation analysis of k-day extreme precipitation over Belgium," *Theoretical and Applied Climatology*, vol. 66, no. 1-2, pp. 117–129, 2000.

[46] Z. L. Li, Z. X. Xu, J. Y. Li, and Z. J. Li, "Shift trend and step changes for runoff time series in the Shiyang River basin, northwest China," *Hydrological Processes*, vol. 22, no. 23, pp. 4639–4646, 2008.

[47] T. Zhao, "Correlation between atmospheric water vapor and diurnal temperature range over China," *Atmospheric and Oceanic Science Letters*, vol. 7, no. 4, pp. 369–379, 2015.

[48] V. C. Klema and A. J. Laub, "The singular value decomposition: its computation and some applications," *IEEE Transactions on Automatic Control*, vol. 25, no. 2, pp. 164–176, 1980.

[49] Y. Ding and Z. Jiang, "Generality of singular valued composition in diagnostic analysis of meteorological field," *Acta Mechanica Sinica*, vol. 54, no. 3, pp. 365–372, 1996 (Chinese).

[50] M. S. J. Harrison, "Rainfall and precipitable water relationsmps over the central interior of South Africa," *South African Geographical Journal*, vol. 70, no. 2, pp. 100–111, 1988.